

1 Assessment of structural sediment connectivity within catchments: 2 insights from graph theory

3 Étienne Cossart¹, Mathieu Fressard¹

4 ¹Université de Lyon (Jean Moulin, Lyon 3), UMR 5600 CNRS – Environnement Ville Société, Lyon, 69007, France

5 *Correspondence to:* Étienne Cossart (etienne.cossart@univ-lyon3.fr)

6 **Abstract.** To describe the sedimentary signal delivered at catchment outlets, many authors now refer to the concept of
7 connectivity. In this framework, the sedimentary signal is seen as an emergent organization of local [links](#) and interactions.
8 The challenge is thus to open the black boxes that remain within a sediment cascade, [which](#) requires both accurate
9 geomorphic investigations in the field (reconstruction of sequences of geomorphic evolution, description of sediment
10 pathways) as well as the development of tools dedicated to sediment cascade [modeling](#). More precisely, the development of
11 tools [devoted](#) to the study of connectivity in geomorphology is still in progress, although graph theory offers promising
12 perspectives (Heckmann and Schwanghart, 2013). In this paper, graph theory is applied to abstract the network structure of
13 sediment cascades, keeping only the nodes (sediment sources, sediment stores, outlet) and links (linkage by a transportation
14 agent), represented as vertices and edges. From the description of the assemblages of sedimentary flows, we provide three
15 main indices to explore how small-scale processes may result in significant broad-scale geomorphic patterns. [The main](#)
16 [hypothesis is that the network structure dictates how sediment inputs from various sources interact at tributary junctions and](#)
17 [finally at the outlet of a cascading system.](#) First, we use the flow index to assess the potential contribution of each node to the
18 sediment delivery at the outlet. Second, we measure the influence of each node regarding how it is accessible from both
19 sediment sources and the outlet (using the Shimbel index). Third, we calculate a connectivity index [revealing](#) whether the
20 potential contribution of a node is lower or higher than expected from its location within the network. These indices are [first](#)
21 [computed](#) for a virtual sediment cascade [and then](#) applied to a catchment located in the southern French [Alps](#). [We](#)
22 [demonstrate that these indices may lead to simulations of sediment transfer and help in identifying the hotspots of](#)
23 [geomorphic change.](#) In the present case, we try to predict how a sediment cascade may be impacted by an edge disruption or
24 a reconnection.

25 1 Introduction

26 The concept of connectivity now provides an overarching framework in geosciences to explore better how catchments
27 function. Connectivity was first defined in ecology to assess the spatial coherence of a system of landscape elements, a
28 coherence that is necessary to maintain or restore ecological functions (Bennett, 2004). Following these pioneering
29 discussions, it has been increasingly used by hydrologists to model hydrological connection patterns (Delahaye et al., 2001;

1 Douvinet et al., 2008). For instance, Ali and Roy (2009) stated that hydrological connectivity can be seen as a function of the
2 available water volume (calculated from a hydrological balance) and the rate of transfer. More recently, connectivity has
3 appeared as a fruitful conceptual framework in geomorphology (Brierley et al., 2006; Wainwright et al., 2011; Fryirs, 2013;
4 Hoffmann, 2015). It helps in studying the spatiotemporal unsteadiness of sediment transport within catchments, and why
5 sediment cascades can be considered a “jerky conveyor belt” (Ferguson, 1981). Unsteadiness patterns in sediment transfers
6 are indeed a major field of research for geomorphologists, and refer to the “spatial and temporal paradox” described by
7 McGuiness et al. (1971): in a catchment, sediment delivery from sources on hillslopes is not correlated with sediment
8 delivery at the outlet. Consequently, sediment cascades are not necessarily efficient in transferring sediments, highlighting a
9 “sediment delivery problem” (Walling, 1983). Finally, geomorphic signals, especially sediment delivery, cannot be
10 interpreted easily (e.g. in terms of climate change, anthropogenic influences, etc.) and may rather reveal a “sedimentological
11 anarchy” (Walker, 1990; Bravard, 1998; Schumm, 2005). At the catchment scale, geomorphic processes may be alternately
12 coupled to create a sediment impulse or antagonistic to create a blockage.

13 Recently, many authors have sought a complex-systems approach to conceptualize the continuum of sediment transfer: how
14 processes, at local scales, may be combined to understand the functioning of the whole sediment cascade (Fryirs et al., 2007;
15 Borselli et al., 2008; Fryirs, 2013; Bracken et al., 2015). Such a multiscale framework was conceptualized by Heckmann
16 and Schwanghart (2013), who clearly distinguished the coupling of processes and connectivity. On the one hand,
17 geomorphic coupling is “the linkage of distinct landforms or landscape units by sediment transport” (Harvey, 2001); it refers
18 to “elementary interactions at the relatively small scale” (Faulkner, 2008). On the other hand, “the degree of coupling, the
19 combined effect of lateral (hillslope to channel) and longitudinal (from one river reach to another) linkages between system
20 components, is termed (sediment) connectivity” (Heckmann and Schwanghart, 2013). Shifting from the local to the
21 catchment scale remains the main issue in explaining how [erosion and sediment transfer on a small spatial scale interact to result in broad-scale geomorphic patterns and processes](#) (Bracken et al., 2015). It requires the development of numerical
22 methods to acquire an exhaustive inventory of all the local linkages within the sediment cascades, to assess their properties,
23 and then to predict the result of their combination at catchment scale. One promising field of research has been opened up by
24 the application of graph theory, [which](#) offers mathematical tools to [analyze](#) statistically the assemblages of all the
25 components of a [sediment cascade](#). It is a [spatially explicit analysis](#) since [nodes](#) and [edges](#) are [spatial objects](#) and since
26 [distance plays a role in the modeling](#) (Heckmann and Schwanghart, 2013; Heckmann et al., 2015). [This mathematical](#)
27 [approach is based on a graph representation of the hydrological network that has been used since decades to describe](#)
28 [watercourses shape and organization](#) (Strahler, 1957; Shreve, 1974). This methodological framework focuses particularly on
29 structural connectivity, i.e. the influence of the spatial patterns [formed](#) by the linkages on sediment delivery. One main
30 objective is to provide a quantitative index that would help in comparing [the skeleton of the sediment cascades](#) in both space
31 and time. It could also be used to [estimate](#) the contribution of a given part of the catchment to provide sediment at the outlet
32 and to [predict](#) where [local erosion should be monitored](#) (Cavalli et al., 2013).

1 In this paper, we propose such a connectivity index. Following a brief state-of-the-art regarding connectivity indices, we
2 explore the main mathematical tools provided by graph theory to measure structural sediment connectivity. We particularly
3 aim to complement the indices already published in order to develop a framework in which geomorphic simulations of
4 changes can be carried out. The proposed connectivity index is first described through a fictive and simple sediment cascade.
5 Then, it is applied to the Celse-Nière study area (French Alps) to explore the spatial patterns of (dis)connectivity within the
6 catchment based on a scenario analysis. Finally, we discuss the main applications and interpretations of the proposed
7 connectivity index.

8 **2 State-of-the-art**

9 By stating that catchments are inefficient at supplying sediment to the outlet, Walling (1983) pointed out a problem that
10 arises from (dis)connectivity. He showed that catchments (especially larger ones) tend to be characterized by a low sediment
11 delivery ratio (SDR).

12
$$SDR = \frac{V_h}{V_o} \quad (1)$$

13 where V_h is the volume of sediment eroded from hillslopes and V_o is the volume of sediment delivered at the outlet of the
14 catchment. The SDR is a synthetic index that provides a proxy to assess the connectivity of a catchment, and allows
15 comparisons in both space and time. Recently, it has been demonstrated that SDR (and connectivity) decreases with
16 increasing landscape morphological complexity (Baartman et al., 2013). One main criticism regarding this index is that
17 catchments remain a black box: no attention is paid to the geomorphic linkages involved at the local scale, or to the
18 feedbacks between geomorphic processes (Gumiere et al., 2011; Fryirs, 2013). In this respect, the SDR has been interpreted
19 as a simple “performance” factor to relate erosion measured at the plot scale to sediment yields observed at the larger scale.
20 Its usefulness has been critically discussed during recent decades (Hoffmann, 2015).

21 To open such black boxes, the concept of connectivity was subdivided into two distinct parts (With et al., 1997; Tischendorf
22 and Fahrig, 2000; Turnbull et al., 2008). On the one hand, structural connectivity refers to spatial patterns in the landscape,
23 such as the spatial distribution of landscape units, which influences sediment transfer patterns and sediment paths. On the
24 other hand, functional connectivity focuses on how geomorphic processes may activate or block the sediment transfer along
25 the spatial links within the sediment cascade (Kimberly et al., 1997; With and King, 1997; Belisle, 2005; Uezu et al., 2005).
26 The latter is now also often called process-based sediment connectivity and was documented in depth in a recent review
27 (Bracken et al., 2015). Here, we focus on structural connectivity, whose quantification is required to explore and understand
28 the responses of geomorphic systems (Wainwright et al., 2011).

1 **2.1 Assessment of structural sediment connectivity**

2 Borselli et al. (2008) and Cavalli et al. (2013) **developed** a connectivity index (Eq. 2) that refers to structural connectivity. It
3 estimates that connectivity at one location within the catchment can be seen as a ratio between an upslope (Eq. 3) and a
4 downslope component (Eq. 4):

5 $IC = \log_{10} \left(\frac{D_{up}}{D_{dn}} \right)$ (2)

6 $D_{up} = \bar{W} \bar{S} \sqrt{A}$ (3)

7 $D_{dn} = \frac{\sum_i d_i}{W_i S_i}$ (4)

8

9 where W is the average weighting factor of the upslope contributing area, S is the average slope gradient of the upslope
10 contributing area (m/m) and A is the upslope contributing area (m^2) and where d_i is the length of the flow path along the i^{th}
11 cell according to the steepest downslope direction (m), and W_i and S_i are the weighting factor and the slope gradient of the i^{th}
12 cell, respectively. In Borselli et al. (2008), the weighting factor W **first** corresponded to the C-factor of USLE-RUSLE
13 models (Wischmeier and Smith 1978; Renard et al. 1997) to refer to frictions that hinder sediment transfer. More recently, it
14 has been demonstrated that topographic surface roughness can provide a good estimation of the weighting factor (Cavalli et
15 al., 2013; Baartman et al., 2013): **a high roughness value is seen as impeding sediment transfer**. This index opens up a
16 fruitful field of research to assess structural connectivity. First, it opens the black boxes within a catchment: the IC can be
17 calculated for each cell of the catchment, **highlighting** **those cells that may contribute greatly**  to the sediment flux at the
18 outlet. Second, this index takes into account all the links between a cell and all other components of the catchment: it nicely
19 refers to the definition of connectivity. Third, the index can be mapped enabling comparisons between various locations (a
20 specific tool has been developed in Arc GIS), and the calculation of maps of connectivity evolution over time  Nevertheless,
21 this index remains empiric, so that comparisons between catchments should be made carefully. **More specifically, while such**
22 **a method helps in identifying specific configurations that are highly susceptible to sediment delivery, it remains difficult to**
23 **provide scenarios of change (e.g. the consequences of land use change, retention basin creation or removal).**

24 **2.2 Graph theory applications to structural connectivity**

25 Another promising field of research is the application of graph theory, which provides a robust mathematical framework for
26 describing networks such as sediment cascades (Heckmann and Schwanghart, 2013; Heckmann et al., 2015; Cossart, 2016).
27 Graph theory is applied to **model a network structure as nodes** (representing sediment sources, sediment stores and the
28 outlet) **connected by edges** (representing linkages by a geomorphological process). Both spatial and topological
29 configurations of the network and the fluxes associated with the respective edges are responsible for the sediment delivery
30 at the outlet (Heckmann and Schwanghart, 2013; Heckmann et al., 2015). The goal is thus to obtain a pattern that can be
31 described by algebraic tools (typology of linkages, identification of local sinks, etc.) to show the overall structure of the

1 sedimentary cascade. Graph theory enables an objective description of the [connections of sedimentary flows](#), and thus an
2 [estimation of the potential influence of the network on the amount of sediment load](#). Indices provided by graph theory have
3 been developed to describe the properties of single landscape units (nodes), sediment pathways (edges) and sediment
4 cascades (edge sequences = paths). The nodes can be characterized by the number and type of links that may provide or
5 [transport](#) sediments. Sediment sources  are characterized by the [absence](#) of input [links](#); sinks are characterized by no output
6 link; and other nodes correspond to [connectors](#) whose importance is revealed by their degree (number of input and/or output
7 links). The links may be characterized by the geomorphic process that carries sediments. Regarding the edge sequences, their
8 main characteristic is whether or not they contribute to the sediment delivery at the outlet: do they correspond to an
9 [independent subcascade](#) or not?

10 [Another application](#) is to carry out “flow analyses”: in a directed graph (such as sediment cascades), each edge has a capacity
11 and each [edge receives a flow](#)  flow must satisfy the restriction that the amount of flow into a node equals the amount of
12 flow out of it  unless it is a source, which has only an outgoing flow, or a sink, which has only an incoming flow. This
13 simulation is based on an assumption of flow conservation, [and is a complementary approach to the assessment of sediment](#)
14 [connectivity](#). In the case of sources with no incoming links, they can be assigned a default common value. Sometimes called
15 the network effect (Pumain and Saint-Julien, 2010; Czuba and Foufoula-Georgiou, 2015), this shows  how the network
16 structure may affect the “potential for creation, persistence, or dispersion of sediment waves” (Gran and Czuba, 2015), and
17 finally the total delivery at the outlet (Czuba and Foufoula-Georgiou, 2015; Cossart, 2016).

18 Nevertheless, these indices do not predict the role of sediment connectivity on sediment delivery, especially in the case of
19 scenarios of changes. New methodological procedures from graph theory need [be](#) developed, so we propose here a brief
20 state-of-the-art of previous studies in which the influence of a spatial network structure on material or immaterial fluxes has
21 been thoroughly explored using graph theory. Although [such studies have focused on geography](#) (Cole and King, 1968;
22 [Gleyze, 2008](#)), [social networks](#) (Freeman, 1979) or, more recently, [ecology](#) (Ludwig et al., 2002; Belisle, 2005), they have
23 developed some metrics and discussed some concepts particularly relevant in geomorphology: the relationship between
24 connectivity and the total amount of fluxes passing through the system, and the identification of local hotspots where any
25 change may have an impact on the whole system (Marra et al., 2014; Czuba and Foufoula-Georgiou, 2014; Czuba and
26 Foufoula-Georgiou, 2015; Masselink et al., 2016). In such studies, one key requirement is to provide a hierarchy of the
27 influence of nodes within the network. Nodes characterized by high connectivity have a considerable influence within a
28 network as they control the fluxes passing between many others. Such high connectivity nodes are also those where a
29 disruption would lead to more serious damage of the network’s functioning (Haggett and Chorley, 1969; Newman, 2010)
30 and may be considered hotspots. They lie on the largest number of possible paths [within the network](#). Many indices provided
31 by graph theory have been applied to undirected graphs (for a review, see Rodrigue, 2017). Such indices are the result of a
32 long procedure of research held by geographers to formalize spatial networks and spatial interactions (Pumain and Saint-
33 Julien, 2010). From their experience we can avoid difficulties and understand how structural connectivity can be measured in
34 directed graphs such as sediment cascades.

1 The Betweenness centrality index (B) measures the extent to which a node i lies on paths between other nodes (Eq. 5):

2
$$B_i = \frac{\sum n_{ijk}}{n_{jk}} \quad (5)$$

3 where n_{ijk} is the number of paths that exist from a node j to a node k, and that pass through i; and where n_{jk} is the total
4 number of paths within the network, from j to k. Such simulation provides a good evaluation of the potential volume that
5 may pass through the nodes and is helpful in interpreting, the real fluxes observed in each node of the network. One main
6 criticism is that this index enhances the role of nodes close to the center of gravity of the network and is not really efficient
7 in ranking the influence of eccentric nodes (Rodrigue, 2017). However, such eccentric nodes are close to the sources of the
8 network so that they should be ranked in relation to their importance in sediment transfer. Furthermore, spatial patterns are
9 taken into account in a simplistic way: the distance (and the friction effect associated to the distance to hinder fluxes) is not
10 considered. We note that distance can be calculated in different ways: it can represent the length of the path, the time
11 necessary to travel along the path, the cost necessary to travel, etc. Consequently, various properties of the edges can be used
12 to approximate the velocity of sediment transfer (Czuba and Foufoula-Georgiu, 2015).

13 The Shimbel index (Shi) takes into account the distance between nodes and considers whether the location of the node
14 increases or decreases the total length of all possible paths within the network (Eq. 6), (Newman, 2010; Rodrigue, 2017). For
15 one node i, it corresponds to the sum of the length of all the shortest paths connecting all other nodes j in the graph (d_{ij}). To
16 facilitate comparisons in both space and time, this index should be normalized, i.e. divided by the sum of the length of all the
17 paths in the network, from j to k (d_{jk}).

18
$$Shi_i = \frac{\sum d_{ij}}{\sum d_{jk}} \quad (6)$$

19 If the Shimbel index is high, then the node contributes to creating long paths within the network (and thus attenuates the
20 compactness of the network). If the Shimbel index is low, then the node maximizes the compactness of the network. This
21 index is much more efficient at ranking the influence of eccentric nodes on the network and can be enriched by considering
22 various types of distance (geodesic, time, etc.). It is considered a very good proxy of accessibility and is thus sometimes
23 called an “accessibility index”. Nevertheless, we should point out that the lower the Shimbel index, the higher the
24 accessibility (and thus the connectivity) of the nodes: while counterintuitive, this feature is now well accepted within the
25 scientific community (Rodrigue, 2017).

26 Both indices enable an in-depth description of the skeleton of a network and highlight the potential impacts of the network
27 structure on flux patterns. They can thus provide conceptual and mathematical frameworks to explore the structure of
28 sediment cascades. Nevertheless, they cannot be applied directly to measure sediment connectivity as sediment cascades are
29 directed graphs, and thus more complicated in terms of mathematical conceptualization.



1 3 Methodology: the Index of Connectivity (IC)

2 From both recent developments on sediment connectivity metrics and past studies on the applications of graph theory to
 3 spatial networks, we now develop a methodological framework focusing on the analysis of sediment transfer within a
 4 network. At the catchment scale, graph theory helps in identifying specific assemblages and, more particularly, some
 5 subcascades that are not connected to each other. It corresponds to connected components, i.e. a subgraph in which nodes are
 6 all connected to each other (Newman, 2010). Their identification may reveal the spatial fragmentation of the sediment
 7 cascade and thus highlight the extent of the active contributing area in terms of sediment delivery at the outlet.

8 At a more local scale, to provide indices that can measure sediment connectivity within the sediment cascade, we have
 9 developed the calculation of the IC (index of connectivity) which is based on (1) potential sediment fluxes and (2)
 10 accessibility (Fig. 1). The objective is to assess spatially the respective influence of each node on sediment connectivity
 11 inside the catchment area.

12 Two nodes i and j are joined or adjacent if there is an edge from i to j . Suppose we are given a directed graph with n nodes,
 13 the graph can be represented by an $n \times n$ adjacency matrix A , constructed as follows: if there is an edge from node i to node
 14 j , then we enter 1 in row i , column j of the matrix A .



15 3.1 Potential flows in directed graphs

16 As in undirected graphs, the first issue is to quantify the “network effect” (according to Pumain and Saint-Julien, 2010) to
 17 highlight how the spatial structure of paths influences the amount of sediment transferred to the outlet. In sediment cascades,
 18 only the paths that come from one node j to the outlet o have to be considered so that in each node i , we have to measure the
 19 extent to which i lies on paths from other nodes j to o (F_{ijo}). This measurement is divided by the total number of paths that
 20 come from all nodes j to o (F_{jo}) to reveal the proportion of the total number of paths that lies on i (Eq. 7).

$$21 F_i = \frac{\sum F_{ijo}}{F_{jo}} \quad (7) \quad \text{Yellow triangle icon}$$

22 F_{ijo} and F_{jo} can be calculated by reconstructing the sediment pathways throughout the cascade. Under the hypothesis of “all
 23 things being equal”, a virtual volume of sediments (1 unit) is set on each node so that a spatially-uniform sediment input is
 24 considered. As suggested by Gran and Czuba (2015) such a theoretical simplification allows the simulation of sediment
 25 wave generation and movement, it exhibits the specific influence of the spatial structure of the network on the sediment
 26 wave pattern. In case of converging flows, the progressive increase of the fluxes is exhibited. In case of diverging flows, the
 27 flow can be subdivided between edges (equally or according to a ratio) so that the complex pattern of sediment wave
 28 generation and movement can also be described. In terms of mathematical procedure, the evacuation of sediment can be
 29 simulated by a multiplication of the adjacency matrix by a matrix representing the sediment sources (S_0) (Eq. 8). This is a
 30 one-column matrix, where each row represents a node of the cascade and the value 1 is entered in each row to represent the
 31 virtual volume of sediments at the beginning of the transfer. Each multiplication corresponds to an iteration, in which each

1 sediment unit is transferred along one edge, according to the links described by the adjacency matrix (Eq. 8 and Fig. 1). The
2 result provides a matrix S_{\perp} highlighting where the sediments are after one single iteration.

3 $S_n = S_{n-1} \times A$ (8)

4 The operation is repeated until all the virtual sediments are evacuated, and the results can be represented within a synthetic
5 matrix (S.), concatenating S_0, S_1, \dots, S_n matrices, obtained during the calculation (Fig. 1).

6 3.2 Accessibility from sources to sinks

7 Within a sediment cascade, the influence of geomorphic units (sources, stores, and sinks) on sediment delivery can be
8 assessed by considering their location inside the cascades. The central hypothesis is that a node whose distance between the
9 sediment sources and the outlet is minimal has a greater influence on the overall sediment cascade. In other words, if such
10 strategic nodes are disconnected from the outlet (i.e. if an edge connecting the strategic nodes is disrupted), the spatial
11 pattern of the transport capacity changes. Not only would the total amount of sediment fluxes change, the “mutual
12 interferences” that occur at such geomorphic hotspots would also be modified (Benda, 2004a; 2004b). Characterizing the
13 nodes by their location within the network refers to the concept of accessibility and is thus very similar to the calculation of
14 the Shimbel index in the case of undirected graphs. In directed graphs, the calculation of the accessibility (Shi) of each node
15 i can be made from a distance matrix D (Eq. 10 and Fig. 1):

16
$$\overline{Shi}_i = \frac{D_{\cdot i} + D_i}{D_{..}} \quad (10)$$

17 where $D_{\cdot i}$ is the total of the distances between i and the nodes (sources and stores) that feed i , D_i is the distance between i and
18 the nodes located downstream, and $D_{..}$ is the total of the distances of all the paths within the network. The main interest of
19 this index is that it enhances the sources (where $D_{\cdot i}$ equals 0) and, more particularly, the sources that minimize the distance
20 to the outlet.

21 3.3 Combination of indices

22 The indices F and Shi provide a quantitative and complementary description of the sediment cascade skeleton: the first
23 reveals the potential proportion of sediment discharge passing through each node; the second measures the proportion of
24 potential paths (from all points within the catchment and the outlet) that lie across each node. Classically, the potential
25 sediment discharge at a node increases in relation to the number of paths that come from sources (i.e. the active contributing
26 area is larger). Nevertheless, due to the geometry of paths, confluences and, more generally, the network structure, there can
27 be some interference in terms of sediment movement through the system: the sediment discharge at a node can be higher or
28 lower than expected from the single number of paths supplying sediments. To estimate this possible under- or
29 overrepresentation of potential sediment volume at each node, a ratio between F and Shi can be calculated (Eq. 11 and
30 Fig. 1):

31
$$IC_i = \frac{F_i}{A_i} \quad (11)$$

1 The expected results can be considered a normalization of the potential sediment fluxes F_i .

2

3 **3.4 Implementation**

4 From a geomorphological map, a graph can be digitalized in GIS software (QGIS), which consists of depicting a regular
5 network of nodes. Each node can be characterized by the geomorphic unit to which it belongs, and the linkages between the
6 nodes can be digitized from geomorphological expertise. The links correspond to directed fluxes, driven by gravity, and we
7 only consider converging flow. To simplify the network structure, each node cannot have two output links. The “Network”
8 QGIS tools can be used to generate the adjacency matrix (as an edge list matrix) and exported to R software. In the latter, the
9 matrix was converted into an origin-to-destination matrix, and the distance matrix was automatically created (a topological
10 distance was considered) using the igraph package. All calculations on matrices were conducted in R, and the results
11 exported to QGIS to be mapped.



12 **4 Results and interpretation**

13 **4.1 Implementation on a virtual catchment**

14 To address the role of network structure in sediment fluxes, a reduced-complexity network is first used. The indices are
15 calculated on a small virtual catchment of 7 nodes and 6 links (Fig. 2a), from the following parameters: the adjacency matrix
16 and the distance matrix (Table 1 and 2). The first model run is parameterized in a simplistic way so that all sources are
17 assumed to be of equal importance, using spatially-uniform sediment inputs (volume availability equals 1 at each node at
18 time 0) and a topological distance (each edge corresponds to a distance of 1 unit).

19 **4.1.1. Potential fluxes**

20 First, a map of the potential fluxes within the sediment cascade can be drawn (Fig. 2b and 2c, Table 3). Such a result can be
21 useful for defining a local monitoring strategy (e.g. survey locations) for sediment transfer and then interpolating local
22 measurements at the catchment scale. Moreover, the F_i index may provide a hierarchy between the nodes by assessing the
23 increase in sediment upstream and downstream of the node. For instance, in our virtual study case, the amount of sediment
24 classically increases downstream, as there is no interruption of the cascade and we only consider converging flow.
25 Nevertheless, the main increase occurs at node D, pointing out that this node is a junction where there is interplay between
26 various tributary systems. D may correspond to a zone of sediment persistence within the catchment, so that any disruption
27 of this node (blockage due to an overflow of sediments, anthropogenic action, etc.) would significantly modify the
28 development of the sediment pulse. However, one main criticism is that the F_i index pays little attention to the sediment
29 sources (here A, B and G), (Fig. 2c). As it corresponds to the initiation zones of the sediment cascade, the events that happen
30 there may influence long pathways to the outlet. As mentioned for the Betweenness index (B), it is necessary to discriminate
31 better the potential influence of sources and stores located next to sources.

32 **4.1.2. Accessibility**

1 The accessibility map can then be computed based on the distance matrix (Fig. 3 and Table 2). Here, G is characterized by
2 better accessibility, greater than A, greater than B: indeed the short distance between G and the outlet suggests it would have
3 a higher influence on sediment delivery. From a geomorphic point of view, it reveals that the time *of* sediment transfer is
4 short *and the possibility of intermediate storage is low*. Figure 3 thus illustrates such a hierarchy of the influence of sediment
5 sources on sediment delivery at the outlet. In terms of management, it highlights the sources that can be activated to cope
6 with sediment exhaustion at the outlet or, conversely, sources where protection strategies should be applied in the case of
7 sediment overflow. *Because of* this issue, this index is not a good proxy of connectivity as it underestimates the role of the
8 outlet and all nodes close to the outlet, and does not pay attention to the confluences between various pathways inside the
9 sediment cascade. At the catchment scale, the roles of D and E are not shown although they are important connectors
10 between pathways developed from sources A and B. The indices of both nodes have to be carefully compared to note that D
11 is closer to different sources and the outlet than E.

12

13 **4.1.3. Index of connectivity (IC)**

14 The IC provides synthetic metrics, suggesting that E and D are the most important geomorphic hotspots (Fig. 4), with very
15 similar values (0.8 and 0.71, respectively). E and D are at confluences and thus lie on various sediment paths from distinct
16 sources. Their potential influence on the whole sediment cascade is high, so that any disruption of these nodes would
17 considerably alter the elementary interactions between many nodes and sediment paths. Consequently, D and E may
18 significantly modify the ability of the cascade to provide sediments and should be further studied in depth to document the
19 functional connectivity or to assess erosional rates (local monitoring, field observations). The outlet F has a quite high index
20 (0.66) but lower than E and D. This value highlights that the connectivity of a node is not proportional to the total volume of
21 sediment that passes through it. In the case of F, the IC is partly influenced by the high potential sediment volume that passes
22 through it but we point out that any disruption at this node would be ambiguous. For example, it would interrupt the
23 sediment delivery but the organization of the three tributary subcascades from sources A, B and G would not be modified.
24 Furthermore, the patterns of mutual interferences at the confluences (E and D) would also remain unmodified, so that
25 sediment pulse generation and movement would not be modified. Consequently, the spatial structure of the cascade network
26 would be roughly unchanged under the hypothesis of F disruption. Regarding the sources (A, B and D), a hierarchy is
27 evidenced. The source G has a greater influence on the sedimentary signal at the outlet due to its proximity (IC = 0.53),
28 which is greater than A and B (IC equals 0.27 and 0.12, respectively).

29

30 **4.1.4. Sensitivity of IC to sediment availability**

31 To investigate how sensitive the indices are to parameterization, we modify the initial conditions of our virtual sediment
32 cascade. Regarding sediment availability, we consider G exhausted (volume equals 0) and B overflowing (volume equals 2).
33 All other nodes remain unchanged. Regarding the distance between E and F, it is now twice the initial value (D_{EF} equals 2),
34 (Fig. 5a and Table 4).

1 To interpret the result we first differentiate nodes whose connectivity increases and nodes whose connectivity decreases. As
2 expected, the potential flow F_i is mainly modified at B whose influence increases (F_B shifts from 0.05 to 0.07), and at G
3 whose influence becomes null (Fig. 5b and Table 4). At other nodes, an increase is observed at D (F_D shifts from 0.18 to
4 0.21) while F_E and F_F remain roughly unchanged (shifting from 0.80 to 0.85 and 0.66 to 0.56, respectively). While the node
5 D was already strategic in the first simulation, the increase in sediment availability at B reinforces its influence on the whole
6 sediment cascade. Downstream, the potential flow at E and F is not reinforced by the amount of sediment delivered at B
7 because of the exhaustion of G.

8 Considering the accessibility (Fig. 5c), the higher eccentricity of F has an impact on A_F but, more generally, alters the
9 accessibility of all nodes. The accessibility coefficient decreases significantly at B: the subcascade organized from B is the
10 longest and all the sediment paths that may exist along this subcascade are impacted by the greater distance between E and F.
11 As a consequence, the outlet is here significantly less accessible from the source B than from the sources A and G (the latter
12 remaining the closer). It can be noticed that the accessibility of D is not impacted by the higher eccentricity of F. A_D remains
13 roughly stable, and even suggests a slight improvement in accessibility. All nodes that are characterized by great centrality,
14 and that are closer to both the sources and the outlet, are not affected by an increasing eccentricity at the margins of the
15 cascade (if the distance from sources, or to the outlet, increases).

16 Finally, regarding the connectivity index (Fig. 5d), the new parameterization modifies the hierarchy of nodes. First, the
17 influence of the confluence nodes increases and, concomitantly, the influence of F decreases. As F is characterized by
18 eccentricity, its influence on the overall system decreases. A disruption would modify the sediment cascade structure less
19 (interplay at tributary junctions, organization of tributary subcascades) than in the previous run model. D here appears as a
20 node of high connectivity as it is close to two main sources and to the outlet. The node E is also of prime importance in terms
21 of connectivity, but its IC value is rather lower than expected from its strategic location. In fact, it is connected to an
22 exhausted source (G). Looking at the sources, a hierarchy is clearly observed: the influence of B increases due to its main
23 contribution to the sediment flow, while the influence of G becomes null as it is exhausted.

24 The IC thus reveals the degree of coupling to both the sources and the outlet for each unit of a sediment cascade. More
25 precisely, it reflects the structural connectivity as it enhances the role of spatial patterns (distance, confluences, etc.) of the
26 network. To make the interpretation easier, a high connectivity node may modify the overall spatial network structure in the
27 case of disruption (e.g. modifications of flux interplay at junctions, creation of independent sediment subcascades
28 unconnected to the outlet, etc.). Moreover, the parameterization could be gradually enriched with geomorphic expertise to
29 pay more attention to sediment availability or to the ability of geomorphic processes to transfer sediment along the paths (i.e.
30 the edges).

31 **4.2 Application to a real sediment cascade**

32 The IC is now applied to a real sediment cascade, whose functioning has already been conceptualized and quantified
33 (Cossart and Fort, 2008; Cossart, 2016).

1 **4.2.1 The Celse-Nière catchment**

2 The Celse-Nière catchment is located in the French Southern Alps, on the eastern flank of the Massif des Écrins (Fig. 6). The
3 current glaciation of this catchment is limited (about 6 km²), in spite of high altitudes (summit approaching 4000 meters at
4 Ailefroide), because this area is partly sheltered from oceanic influences due to its eastward location. For instance,
5 precipitation is about 995 mm.yr⁻¹ at Pelvoux (1280 meters), which is significantly lower than on the western flank of the
6 Massif des Écrins (1195 mm.yr⁻¹ at Valjouffrey, 1160 meters). The equilibrium line altitude ranges from 3000 to 3200 m
7 (Cossart, 2005), which is 200 meters higher than in the western part of the massif.

8 We focus here on the headwater (about 10 km², from 2500 m.asl to 3850 m.asl), which is still occupied by glaciers. Some
9 small tributaries converge into the upper part of the catchment (Ailefroide, Coup de Sabre) as their mouth is blocked by the
10 Sélé glacier valley tongue. Such small catchments are occupied by cirque glaciers, which lie just below granitic and gneissic
11 free-faces and provide both sediments and meltwater to the valley floor. Special attention has already been given to the
12 linkages between the glacial margins and the glacio-fluvial systems (Cossart, 2004, 2016). The presence of morainic ridges
13 still interrupts the sedimentary cascade system, thus forcing local aggradation and change in the glacio-fluvial pattern (Fig.
14 6). Such a complex assemblage makes this area particularly suitable for assessing connectivity and simulating the impacts of
15 new blockages or, conversely, some reconnections.

16 **4.2.2 The structure of the network**

17 As in the virtual case study, a reduced-complexity network model is considered to address the role of the network's spatial
18 structure (Fig. 7). The initial conditions of run 1 of the model are (1) a spatially-uniform sediment input (volume availability
19 equals 1 at each node at time 0) and (2) topological distance is considered (each edge corresponds to a distance of 1 unit).

20 First, it can be noticed that only 56% of all the paths are connected to the outlet while the others are connected to permanent
21 sinks. Twenty-five connected components are identified, highlighting a high fragmentation of the system: only 6 of these
22 encompass more than 10 nodes (including the main connected component connected to the outlet) and 11 encompass fewer
23 than 5 nodes. By applying the typology established by Fryirs et al. (2007), disconnections are due to barriers, buffers and
24 blankets (Fig. 7a). Barriers are here mostly due to moraines: lateral moraines may affect the longitudinal coupling of
25 processes, especially the coupling between glacio-fluvial streams from the cirque glaciers and the mainstem. In that case, the
26 node that corresponds to the upper part of the moraine is a sink, the node corresponding to the downslope part of the moraine
27 is a source, but there is no link between these both nodes.

28 Buffers correspond to moraines, where they decouple scree deposits from the mainstem (scree deposition is forced by the
29 morainic ridge), but also roches-moutonnées and glacio-fluvial terraces. Blankets correspond to scree deposits made of large
30 grain-size boulders that cannot be removed by fluvial processes. Second, the IC highlights the influence of the trunk valley
31 located between the margin of the Glacier-du-Sélé and the confluence with the Coup-de-Sabre proglacial river where high-
32 connectivity nodes are observed (Fig. 6A). This means that potential sediment fluxes are higher than expected from the

1 active contributing areas upstream, so that the network may develop here some zones of potential sediment persistence
2 within the catchment. Furthermore, such nodes correspond to tributary junctions between the main subcascades of the
3 system. The mutual interference may here have an influence on the generation of sediment pulse, and thus on its evolution
4 (transfer to the outlet), as well as on the tributary subcascades located upstream. Sediment persistence, an aggradation pattern
5 in these zones, may generate a retrogressive aggradation that may modify the functioning of subcascades (e.g. decrease in
6 sediment transfer along subcascades in the case of impoundment). For these reasons, such nodes can be considered hotspots
7 of geomorphic change, which can propagate a perturbation along the whole cascade due to a geomorphic change, and thus
8 modify the overall functioning of the system. A significant input of sediments (due, for instance, to a hydro-meteorological
9 event) in these areas would increase the sediment delivery at the outlet and may also alter the ability of tributaries to deliver
10 sediments. The IC also exhibits a hierarchy between the sources. As they are closer to the outlet, all the sources located in
11 the Coup-de-Sabre subcatchment have a greater influence on sediment delivery than the sources located in the Ailefroide,
12 Sélé or Boeufs-Rouges areas.

13 Thus, the map of the IC helps to conceptualize the continuum of sediment transfer and to predict the downstream transfer
14 and delivery of sediment fluxes measured at one point (not necessarily at the outlet). Node connectivity may need to be
15 examined to establish sampling strategies for small-scale measurements of erosion in the field. Furthermore, this first
16 examination highlights that the potential impacts of external drivers (anthropogenic impact, hydro-meteorological event and,
17 more generally, climate change) are space-dependent: the impacts may be greater and efficiently propagated if they affect
18 high-connectivity areas.

19 4.2.3 What if...?

20 The connectivity hierarchy between nodes can be interpreted as the potential influence of the node on sediment delivery and
21 the overall functioning of the cascade. The IC and, more generally, tools provided by graph theory enable the simulation of
22 scenarios to predict which events would have more impact on the cascade. Two other model scenarios were applied here in
23 R to simulate the consequences of a local disconnection and a local reconnection. Run 2 corresponds to an algorithm that
24 tests which edge removal would have the greatest impact on sediment connectivity (i.e. the largest decrease in connectivity
25 at the node characterized by the highest connectivity), (Fig. 7b). This simulation could reflect the possible impact of an
26 anthropogenic feature (e.g. a dam) or a hillslope process (e.g. a dam created by a landslide mass or a debris flow). Run 3
27 (Fig. 7c) corresponds to an algorithm that tests which creation of a new edge would lead to the greatest improvement in
28 connectivity (i.e. where can we create the highest increase in the IC value at a node?). This simulation could reflect the
29 disruption of a barrier or the removal of a blanke for instance following a high magnitude geomorphic event.

30 Run 2 highlights that the greatest impact would occur if the edge located at the toe of the Glacier du Sélé was disrupted. It
31 would lead to the disconnection from the outlet of the main subcascade (fed by Sélé sediment sources) so that only 40% of
32 the nodes would remain connected to the outlet (against 56% in the initial stage). Nevertheless, the modification of the whole
33 system is not just a question of sediment delivery at the outlet. First, we point that that it may provoke an attenuation of the

1 peak of the sediment wave if we compare the simulated sedimentographs between runs 1 and 2 (Fig. 8). Second, the
2 disruption creates a subdivision of the sediment cascade connected to the outlet into two main connected components of
3 quite similar size. The connected component that becomes disconnected from the outlet after run 1 (Boeufs-Rouges area)
4 encompasses 72 nodes, and the other (still connected to the outlet) 142 nodes. Any other edge removal would lead to a new
5 connected component of a smaller size (<72 nodes). The disruption would be more significant than that of an edge located at
6 the confluence with the Coup-de-Sabre proglacial river. In this latter case, many nodes would be disconnected from the
7 outlet, but the three subcascades of Ailefroide, Sélé and Boeufs-Rouges would be less impacted and would still be self-
8 organized within a large connected component. As a result, the structure of the sediment cascade would be less fragmented.
9 Finally, the IC shows where a local disruption may split two connected components of quite similar size, which may have a
10 strong impact in terms of geomorphic functioning. As many geomorphic processes are scale-dependent, some variables
11 influencing sediment transfer that are interdependent at one scale may well be independent at another (Schumm, 2005). A
12 corollary is that the split of a cascade into two connected components (whose sizes are approximately half that of the initial
13 cascade) may modify the scale at which geomorphic processes or controls act and markedly change the functioning of the
14 system.

15 For run 3, a new edge is added to improve the overall sediment connectivity (Fig. 6C). In this case, a link between the
16 Guyard subcatchment and the trunk valley would create the highest IC value at the confluence. Such an increase is due to the
17 large number of nodes (64%) that would become connected to the outlet. Furthermore, these nodes (especially the sources)
18 are relatively close to the outlet, so that the sediment wave exhibits an increase at the beginning of the pulsation (Fig. 8). A
19 reconnection of the subcascade in the Ailefroide area would have a lesser impact because of its eccentricity. It can be noticed
20 that the reconnection of the Guyard subcascade would decrease the influence of the Coup-de-Sabre subcascade on the overall
21 network: in this scenario of reconnection, all the sources of this area are affected by a decrease in IC. According to this new
22 cascade structure, the hierarchy of sources would be modified: the sources of the Guyard area would have a greater influence
23 than the Coup-de-Sabre sources, which would have a greater influence than the Ailefroide, Sélé and Boeufs-Rouges sources.
24 The IC provides an exploration of the cascade structure and may explain to what extent a small-scale modification
25 (disruption of a node, creation of a linkage) may result in significant changes in broad-scale geomorphic patterns and
26 processes. In the present examples, it can also predict the potential impacts on the sediment wave pattern (Fig. 8). More
27 generally, the IC enables comparisons between different states of connectivity within the same catchment.

28 **5 Discussion**

29 Several papers have already addressed the question of the assessment of connectivity (Borselli et al., 2008; Cavalli, 2013;
30 Czuba and Foufoula-Georgiu, 2015; Gran and Czuba, 2015; Hoffmann, 2015) so we discuss here the potential improvements
31 offered by graph theory. Following Heckmann and Schwanghart (2013), a graph provides both a geometric and an algebraic
32 description of the sediment cascade network. By identifying the connected components within the system, the examination

1 of the geometry of the graph first helps to assess the SDR at the catchment scale and to identify the recurrent types of
2 process coupling. In detail, it aims to determine the interaction of processes that are (in)efficient within the cascade at
3 supplying sediments to the outlet. From the case studies developed here, we also highlight how an algebraic framework may
4 help in exploring how the cascading system functions. Reduced-complexity network models associated with simple
5 hypotheses (spatially-uniform sediment inputs, simple assessment of the distance between nodes based on a topological
6 distance) highlight the zones of greater sediment persistence, where sediment may accumulate in the network. Consequently,
7 the role of the network's spatial structure in the generation of a sediment wave can be simulated and the associated
8 sedimentograph can help in deciphering what is really due to external boundary conditions in sediment delivery variability at
9 the outlet (Fryirs, 2017). Another result is the rank assessment of the geomorphic importance of the nodes, considering their
10 location within the catchment. Following previous authors (Cavalli et al., 2013; Czuba and Foufoula-Georgiu, 2015; Gran
11 and Czuba, 2015), the IC identifies some specific zones that correspond to hotspots of geomorphic change due to their
12 strategic location closer to the sources and the outlet. One main improvement in the graph theory framework is that the
13 algebraic description helps in developing simulation scenarios, while the associated algorithms show the properties of such
14 geomorphic hotspots. They not only influence the total amount of sediment that is delivered at the outlet but they also reveal
15 where disconnections or reconnections may have a strong impact on the organization of the sediment cascade. A
16 disconnection occurring at a hotspot may split the cascade into connected components of quite similar size, modifying the
17 sedimentograph pattern, and may break the organization of path sequences.

18 Such a focus on the spatial dependence of geomorphic processes should be complemented, and the graph can be gradually
19 enriched to take into account more complexity. A geomorphic hierarchy of sources (in terms of sediment supply) can be
20 parameterized: for instance, if a **source** overflows or, conversely, is exhausted. The matrix representing the sediment sources
21 can then be adjusted. Second, distance is an important parameter that can modify the results of A_i , and thus IC_i . Distance
22 involves friction, which hampers the sediment transfer: the greater the distance, the higher the potential friction opposing
23 sediment delivery (i.e. the transfer time increases). Many other kinds of distance can be taken into account, such as the
24 Euclidian distance, but in geomorphology other types of distance may be more relevant. For example, a distance expressed
25 as a time, to reveal the **duration of sedimentary transfer** from one unit to another, can be particularly appropriate, although
26 difficult to assess. A cost distance can also be relevant. By revealing how hampered (or efficient) the sediment transfer is
27 along the edge, a **manning** coefficient, or more generally a roughness index (Baartman et al., 2013)  can be a good proxy of
28 the friction that hampers the sediment transfer. Such parameters can be calculated from high-resolution DEM, combined
29 with the edge characteristics through GIS procedures, and finally integrated within the matrices necessary for the
30 calculations. In this way, graph theory provides a methodological framework that can be extensively enriched by various
31 parameters to reveal the transport capacity, and consequently the potential interplay between network geometry and spatial
32 patterns of transport. One perspective of research is to complement this approach by a more dynamic modelling of the
33 sediment cascade network structure. It is well-known that the assemblages of links and nodes may evolve in accordance with
34 various external forces (e.g., climate, human practices, tectonics). For instance, agent-based models can be suitable to predict

1 the possible evolution of the structure, by considering negative and/or positive feedbacks along the edges (Reulier et al.,
2 2016).

3 **6 Conclusion**

4 This paper seeks to develop an original methodology dedicated to the study of [sedimentary cascades under the hypothesis](#)
5 [that the influence of connectors and paths on sediment](#) delivery is space-dependent. The methods rely on graph theory to
6 assess structural connectivity: the sediment cascade is described as a network and consequently as a graph. Inspired by
7 indices developed in other sciences (transportation science, sociology, ecology), a potential flow and an accessibility of
8 geomorphic units (i.e. accessibility to sediment sources and to the outlet) can be measured throughout the sediment cascade.
9 Both indices are combined to estimate a connectivity index, which reveals how influential a node is within a sediment
10 cascade. Specific applications were implemented in GIS software (QGIS) as well as in software dedicated to data analysis
11 and [matrix](#) calculations (R).

12 The application on a simple virtual catchment and then on a real catchment [shows how the network spatial structure](#) may
13 lead (or not) to sediment mobilization and exportation, from the upper slopes to the outlet of watersheds. The behavior of
14 sediment cascades appears space-dependent: the geometry of paths and the location of nodes have a direct influence on
15 structural connectivity and thus on the ability of the sediment cascade to deliver sediments. As a consequence, some hotspots
16 of geomorphic change can be identified within the catchment. The impact of an external force on the sediment cascade
17 depends on the location of its action: the higher the connectivity of the node, the higher the impact on the cascade. Moreover,
18 some simulations can be [conducted](#) to predict how local perturbations may have an impact on the overall cascade.

19 This issue ([characterizing sediment connectivity at the catchment scale](#)) is one of the main challenges in geomorphology and
20 may help in understanding how a sediment wave develops and moves downstream. In detail, it may be possible to decipher
21 better if sediment pulses reveal the spatial network structure or external boundary conditions (e.g. climate change,
22 anthropogenic pressure, tectonics). [Such results are of importance for management issues](#), for instance in the discussion of
23 the location of a retention basin for sediments in a context of severe erosion, or where sediment continuity should be restored
24 to cope with sediment exhaustion in some rivers.

25

26 **References**

27 Ali, G.V. and Roy, A.G.: Revisiting hydrologic sampling strategies for an accurate assessment of hydrologic connectivity in
28 humid temperate systems. *Geography Compass* 3, 350–374, 2009
29 Baartman, J.E.M., Masselink, R., Keesstra, S.D. and Temme, A.J.A.M.: Linking landscape morphological complexity and
30 sediment connectivity. *Earth Surface Processes and Landforms* 38, 1457–1471, 2013.

- 1 Belisle, M.: Measuring landscape connectivity: the challenge of behavioural landscape ecology. *Ecology* 86, 1988–1995,
2 2005.
- 3 Bennett, G.: Integrating biodiversity conservation and sustainable use. Lessons learned from ecological networks. *World
4 Conservation Union (IUCN)*, Gland, Switzerland, 2004.
- 5 Benda, L.E.E., Andras, K., Miller, D., and Bigelow, P.: Confluence effects in rivers: interactions of basin scale, network
6 geometry, and disturbance regimes. *Water Resources Research*, 40(5), 1-15, 2004a.
- 7 Benda, L.E.E., Poff, N. L., Miller, D., Dunne, T., Reeves, G., Pess, G., and Pollock, M.: The network dynamics hypothesis:
8 how channel networks structure riverine habitats. *BioScience*, 54(5), 413-427, 2004b.
- 9 Brierley, G., Fryirs, K. and Jain, V.: Landscape connectivity: the geographic basis of geomorphic applications. *Area* 38(2),
10 165–174, 2006.
- 11 Borselli, L., Cassi, P. and Torri, D.: Prolegomena to sediment and flow connectivity in the landscape: a GIS and field
12 numerical assessment. *Catena* 75, 268-277, 2008.
- 13 Bracken, L.J., Turnbull, J., Wainwright, J. and Bogaart, P.: Sediment connectivity: a framework for understanding sediment
14 transfer at multiple scales. *Earth Surface Processes and Landforms* 40(2), 177-188, 2015.
- 15 Bravard, J.P.: Le temps et l'espace dans les systèmes fluviaux, deux dimensions spécifiques de l'approche
16 géomorphologique. *Annales de Géographie* 107(599), 3-15, 1998.
- 17 Cavalli, M., Trevisani, S., Comiti, F. and Marchi, L.: Geomorphometric assessment of spatial sediment connectivity in small
18 Alpine catchments. *Geomorphology* 188, 31-41, 2013.
- 19 Chorley, R.J. and Kennedy, B.A. *Physical Geography: A Systems Approach*. Prentice-Hall International, London, 370 pp,
20 1971.
- 21 Cole, J.P. and, King C.A.M.: *Quantitative Geography: Techniques and theories in geography*, Wiley, New York, 471 pp,
22 1968.
- 23 Cossart, É: La recrudescence de l'activité torrentielle dans un bassin versant en cours de déglaciation au cours du XXe
24 siècle. *Géomorphologie: relief, processus, environnement* 3, 225-240, 2004.
- 25 Cossart, É. and Fort, M.: Sediment release and storage in early deglaciated areas: Towards an application of the exhaustion
26 model from the case of Massif des Écrins French Alps since the Little Ice Age. *Norsk Geografisk Tidsskrift – Norwegian
27 Journal of Geography* 62, 115-131, 2008.
- 28 Cossart, É.: L'(in)efficacité géomorphologique des cascades sédimentaires en question: les apports d'une analyse réseau.
29 *Cybergeo: European Journal of Geography* 778, DOI: 10.4000/cybergeo.27625, 2016.
- 30 Czuba, J. A., & Foufoula-Georgiou, E.: A network-based framework for identifying potential synchronizations and
31 amplifications of sediment delivery in river basins. *Water Resources Research*, 50(5), 3826-3851, 2014.
- 32 Czuba, J. A., & Foufoula-Georgiou, E.: Dynamic connectivity in a fluvial network for identifying hotspots of geomorphic
33 change. *Water Resources Research*, 51(3), 1401-1421, 2015

- 1 Delahaye, D., Guermond, Y. and Langlois, P.: Spatial interaction in the run-off process. *Cybergeo: European Journal of*
2 *Geography* 213, DOI: 10.4000/cybergeo.3795, 2001.
- 3 Douvinet, J., Delahaye, D. and Langlois, P.: Modélisation de la dynamique potentielle d'un bassin versant et mesure de son
4 efficacité structurelle. *Cybergeo: European Journal of Geography* 412, DOI: 10.4000/cybergeo.16103, 2008.
- 5 Faulkner, H.: Connectivity as a crucial determinant of badland geomorphology and evolution. *Geomorphology* 100(1-2), 91-
6 103, 2008.
- 7 Ferguson, R.I.: Channel forms and channel changes. In: Lewin, J. (Ed.) *British Rivers*. Allen and Unwin, London. pp. 90-
8 125, 1981.
- 9 Freeman, L.C.: Centrality in social networks conceptual clarification. *Social networks* 1(3), 215–239, 1979.
- 10 Fryirs, K. A.: River sensitivity: A lost foundation concept in fluvial geomorphology. *Earth Surface Processes and*
11 *Landforms*, 42(1), 55-70, 2017.
- 12 Fryirs, K.: DisConnectivity in catchment sediment cascades: a fresh look at the sediment delivery problem. *Earth Surface*
13 *Processes and Landforms Landforms* 38, 30–46, 2013.
- 14 Fryirs, K., Brierley, G.J., Preston, N.J. and Kasai, M.: The disconnectivity of catchment-scale sediment cascades. *Catena*, 70,
15 49-67, 2007.
- 16 Gleyze, J.F.: Effets spatiaux et effets réseau dans l'évaluation d'indicateurs sur les nœuds d'un réseau d'infrastructure.
17 *Cybergeo: European Journal of Geography* 370, DOI: 10.4000/cybergeo.5532, 2008.
- 18 Gumièvre, S.J., Le Bissonnais, Y., Raclot, D. and Cheviron, B.: Vegetated filter effects on sedimentological connectivity of
19 agricultural catchments in erosion modelling: a review. *Earth Surface Processes and Landforms* 36, 3–19, 2011.
- 20 Haggett, P. and Chorley, R.J.: Network analysis in geography, Edward Arnold, Science, 348 pp, 1969.
- 21 Harvey, A.M.: Coupling between hillslopes and channels in upland fluvial systems: implications for landscape sensitivity,
22 illustrated from the Howgill Fells, northwest England. *Catena* 42, 225-250, 2001.
- 23 Heckmann, T. and Schwanghart, W.: Geomorphic coupling and sediment connectivity in an alpine catchment - exploring
24 sediment cascades using graph theory. *Geomorphology* 182, 89-103, 2013.
- 25 Heckmann, T., Schwanghart, W. and Phillips, J.D.: Graph theory: Recent developments of its application in geomorphology.
26 *Geomorphology* 243, 130-146, 2015.
- 27 Hoffmann, T.: Sediment residence time and connectivity in non-equilibrium and transient geomorphic systems. *Earth*
28 *Science Reviews*, 150, 609-627, 2015.
- 29 Kimberly, A.W., Gardner, R.H. and Turner, M.G.: Landscape connectivity and population distributions in heterogeneous
30 environments. *Oikos* 78, 151–169, 1997.
- 31 Ludwig, J.A., Eager, R.W., Bastin, G.N., Chewings, V.H. and Liedloff, A.C.: A leakiness index for assessing landscape
32 function using remote sensing. *Landscape Ecology* 17, 157–171, 2002.

- 1 Marra, W. A., Kleinhans, M. G., and Addink, E. A.: Network concepts to describe channel importance and change in
2 multichannel systems: test results for the Jamuna River, Bangladesh. *Earth Surface Processes and Landforms* 39, 766-778,
3 2014.
- 4 Masselink, R. J., Heckmann, T., Temme, A. J., Anders, N. S., Gooren, H., and Keesstra, S. D.: A network theory approach
5 for a better understanding of overland flow connectivity. *Hydrological Processes* 31, 207-220, 2017.
- 6 McGuinness, J.L., Harrold, L.L. and Edwards, W.M.: Relation of rainfall energy streamflow to sediment yield from small
7 and large watersheds. *Journal of Soil and Water Conservation* 26, 233-235, 1971.
- 8 Newman, M.E.J.: Networks: An Introduction, Oxford University Press, 2010.
- 9 Pumain, D. and Saint-Julien T.: Analyse spatiale : les localisations, Cursus, Armand Colin, Paris, 192 pp, 2010.
- 10 Renard, K., Foster, G.R., Weessies, G.A., McCool, D.K. and Yodler, D.C. Predicting soil erosion by water: a guide to
11 conservation planning with the Revised Universal Soil Loss Equation (RUSLE). U.S. Department of Agriculture.
12 Agriculture Handbook 703, 1-384, 1997.
- 13 Reulier, R., Delahaye, D., Caillault, S., Viel, V., Douvinet, J. and Bensaid, A.: Mesurer l'impact des entités linéaires
14 paysagères sur les dynamiques spatiales du ruissellement: une approche par simulation multi-agents. *Cybergéo* . European
15 Journal of Geography [On line], Systèmes, Modélisation, Géostatistiques, document 788, 2016.
- 16 Rodrigue, J.P.: Geography of transport system, New-York, Routledge, 441 p, 2017.
- 17 Schumm, S.: River variability and complexity, Cambridge University Press, 219 p, 2005.
- 18 Shreve, R. L.: Variation of mainstream length with basin area in river networks. *Water Resources Research* 10, 1167-1177,
19 1974.
- 20 Strahler, A. N.: Quantitative analysis of watershed geomorphology. *Eos, Transactions American Geophysical Union*, 38,
21 913-920, 1957.
- 22 Tischendorf, L. and Fahrig, L.: How should we measure landscape connectivity? *Landscape Ecology* 15, 633–641, 2000.
- 23 Turnbull, L., Wainwright, J., Brazier, R.E.: A conceptual framework for understanding semi-arid land degradation:
24 ecohydrological interactions across multiple-space and time scales. *Ecohydrology* 1, 23–34, 2008.
- 25 Uezu, A., Metzger, J.P. and Vielliard, J.M.E.: Effects of structural and functional connectivity and patch size on the
26 abundance of seven Atlantic forest bird species. *Biological Conservation* 123, 507–519, 2005.
- 27 Viel, V.: Analyse spatiale et temporelle des transferts sédimentaires dans les hydrosystèmes normands. Exemple du bassin
28 versant de la Seulles. Ph-D Thesis, Université de Caen, 382 pp, 2012.
- 29 Wainwright, J., Turnbull, L., Ibrahim, T.G., Lexartza-Artza, I., Thornton, S.F. and Brazier, R.E.: Linking environmental
30 regimes, space and time: interpretations of structural and functional connectivity. *Geomorphology*, 126: 387–404, 2011.
- 31 Walker, R.G.: Perspective, facies modelling and sequence stratigraphy. *Journal of Sedimentary Petrology* 60, 777-786, 1990.
- 32 Walling, D.E.: The sediment delivery problem. *Hydrology*, 69, 209-237, 1983.
- 33 Wischmeier, W.H. and Smith, D.D.: Predicting Rainfall Erosion Losses - A Guide to Conservation Planning. U.S.
34 Department of Agriculture. Agriculture Handbook 537, 1-58, 1978.

1 With, K.A., Gardner, R.H. and Turner, M.G.: Landscape connectivity and population distributions in heterogeneous
2 environments. *Oikos* 78, 151–169, 1997.
3

1

| | | Destination node | | | | | | |
|-------------|---|------------------|---|---|---|---|---|---|
| | | A | B | C | D | E | F | G |
| Origin node | A | 1 | 0 | 0 | 1 | 0 | 0 | 0 |
| | B | 0 | 1 | 1 | 0 | 0 | 0 | 0 |
| | C | 0 | 0 | 1 | 1 | 0 | 0 | 0 |
| | D | 0 | 0 | 0 | 1 | 1 | 0 | 0 |
| | E | 0 | 0 | 0 | 0 | 1 | 1 | 0 |
| | F | 0 | 0 | 0 | 0 | 0 | 1 | 0 |
| | G | 0 | 0 | 0 | 0 | 1 | 0 | 1 |

2 Table 1: Adjacency matrix of the virtual sediment cascade

3

| | | Destination node | | | | | | | | |
|-------------|-------|------------------|---|---|---|----|----|---|-------|-------|
| | | A | B | C | D | E | F | G | D_i | A_i |
| Origin node | A | 0 | 0 | 0 | 1 | 2 | 3 | 0 | 6 | 0.17 |
| | B | 0 | 0 | 1 | 3 | 4 | 5 | 0 | 13 | 0.37 |
| | C | 0 | 0 | 0 | 2 | 3 | 4 | 0 | 9 | 0.29 |
| | D | 0 | 0 | 0 | 0 | 1 | 2 | 0 | 3 | 0.26 |
| | E | 0 | 0 | 0 | 0 | 0 | 1 | 0 | 1 | 0.34 |
| | F | 0 | 0 | 0 | 0 | 0 | 0 | 0 | 0 | 0.49 |
| | G | 0 | 0 | 0 | 0 | 1 | 2 | 0 | 3 | 0.09 |
| | D_i | 0 | 0 | 1 | 6 | 11 | 17 | 0 | 35 | |

4 Table 2: Distance matrix (origin-to-destination) of the virtual sediment cascade. On the right, the rows detail the calculation of the
5 accessibility index.

6

7

8

9

10

11

12

| | | Model iteration | | | | | | | | |
|------|---|-----------------|---|---|---|---|-------|-------------|------|--|
| | | 0 | 1 | 2 | 3 | 4 | 5 | $F_{j_0}^i$ | Fi | |
| Node | A | 1 | 0 | 0 | 0 | 0 | 0 | 1 | 0.05 | |
| | B | 1 | 0 | 0 | 0 | 0 | 0 | 1 | 0.05 | |
| | C | 1 | 1 | 0 | 0 | 0 | 0 | 2 | 0.09 | |
| | D | 1 | 2 | 1 | 0 | 0 | 0 | 4 | 0.18 | |
| | E | 1 | 2 | 2 | 1 | 0 | 0 | 6 | 0.27 | |
| | F | 1 | 1 | 2 | 2 | 1 | 0 | 7 | 0.32 | |
| | G | 1 | 0 | 0 | 0 | 0 | 0 | 1 | 0.05 | |
| | | | | | | | Total | 22 | | |

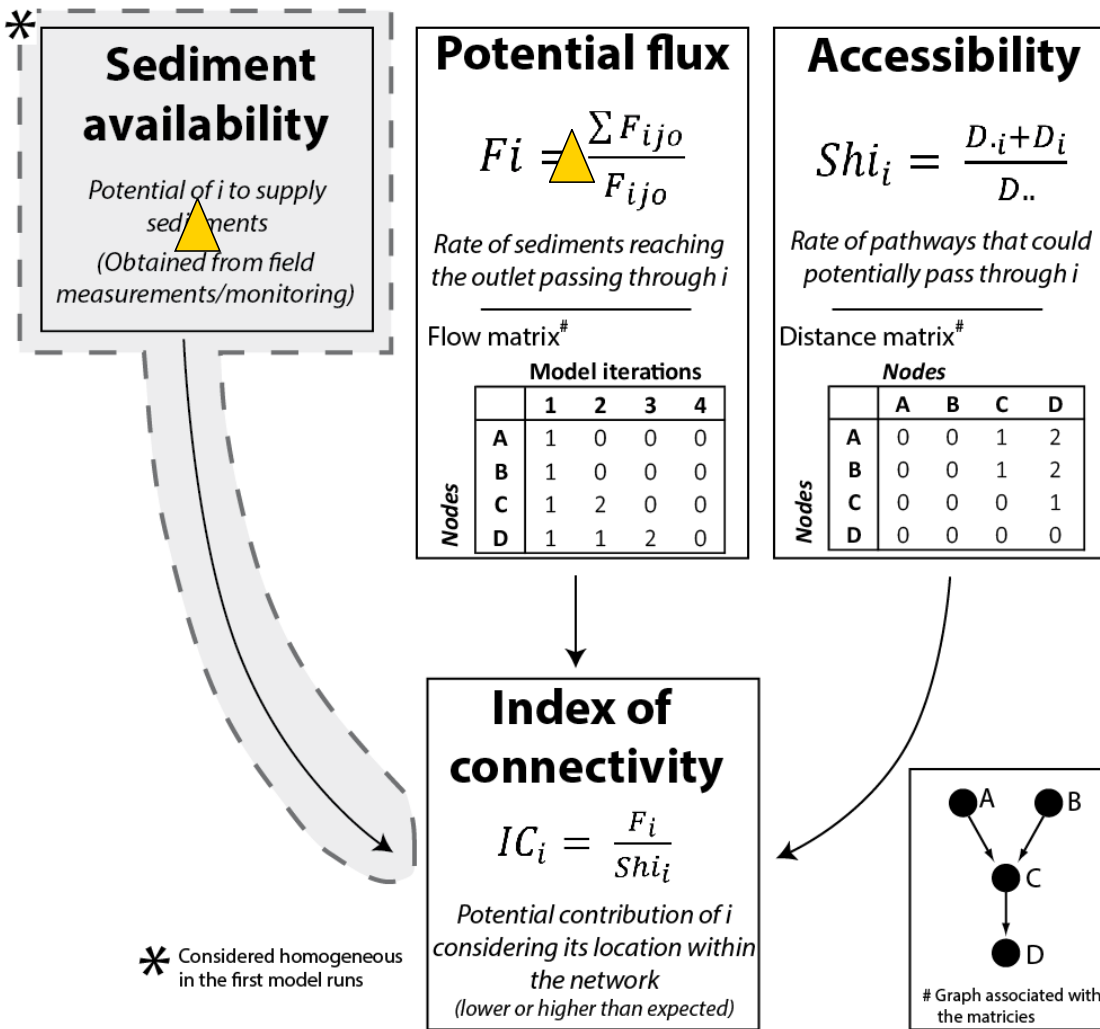
1 Table 2: Analysis of the potential sediment flow within the sediment cascade. The first rows correspond to the iterations simulating
 2 the evacuation of sediments. On the right, the rows detail the calculation of the flow index.

3
4

| | | Model Iteration | | | | | | | | | | |
|------|---|-----------------|---|---|---|---|-------|-------------|------|------|------|--|
| | | 0 | 1 | 2 | 3 | 4 | 5 | $F_{j_0}^i$ | Fi | Ai | ICi | |
| Node | A | 1 | 0 | 0 | 0 | 0 | 0 | 1 | 0.03 | 0.18 | 0.20 | |
| | B | 2 | 0 | 0 | 0 | 0 | 0 | 2 | 0.07 | 0.35 | 0.20 | |
| | C | 1 | 2 | 0 | 0 | 0 | 0 | 3 | 0.10 | 0.28 | 0.38 | |
| | D | 1 | 2 | 3 | 0 | 0 | 0 | 6 | 0.21 | 0.25 | 0.83 | |
| | E | 1 | 2 | 2 | 3 | 0 | 0 | 8 | 0.28 | 0.33 | 0.85 | |
| | F | 1 | 1 | 2 | 2 | 3 | 0 | 9 | 0.31 | 0.55 | 0.56 | |
| | G | 0 | 0 | 0 | 0 | 0 | 0 | 0 | 0.00 | 0.08 | 0.00 | |
| | | | | | | | Total | 29 | | | | |

5 Table 4: Analysis of the potential flow and calculation of connectivity following a new parameterization. The rows indicate the
 6 patterns of sediment evacuation at each iteration of the simulation. Source B provides twice as many sediments and the distance
 7 between E and F is twice that during the initial conditions.

8
9



1

2 Figure 1: Overview of the main parameters used to build the Index of Connectivity (equation details can be found in section
3 3)

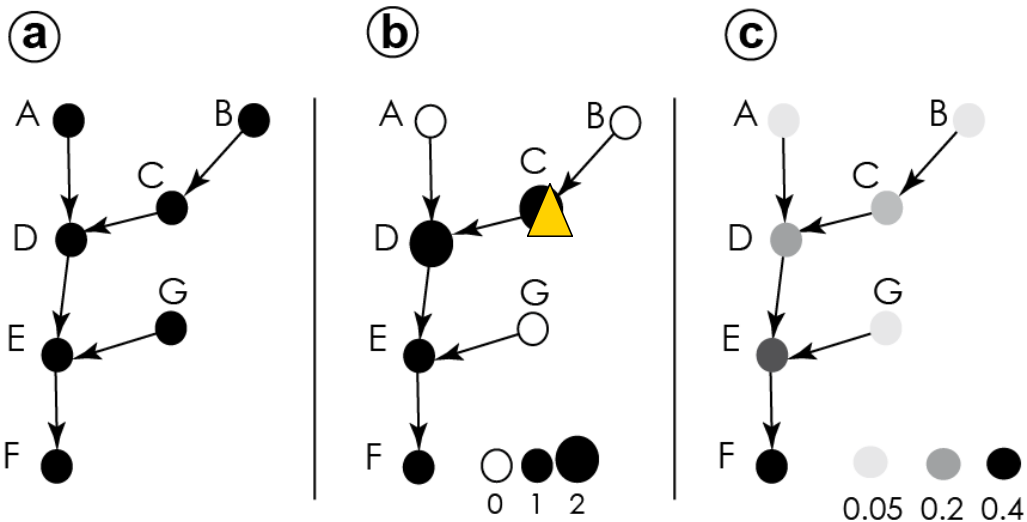


Figure 2: The virtual sediment cascade. a: The structure of the cascade, represented by a graph; b: The potential flow of sediments after one iteration during the simulation; c: Map of flow index values.

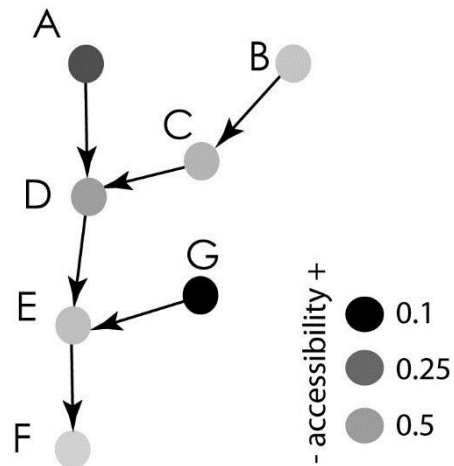
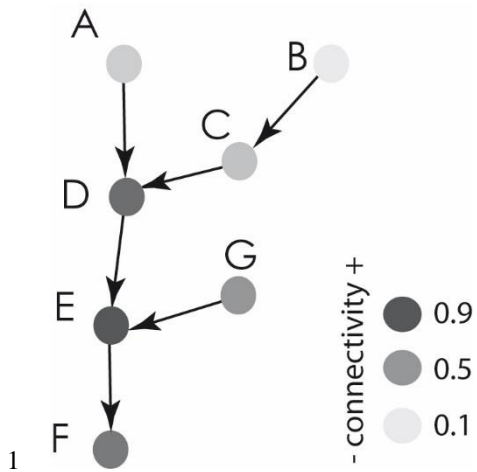
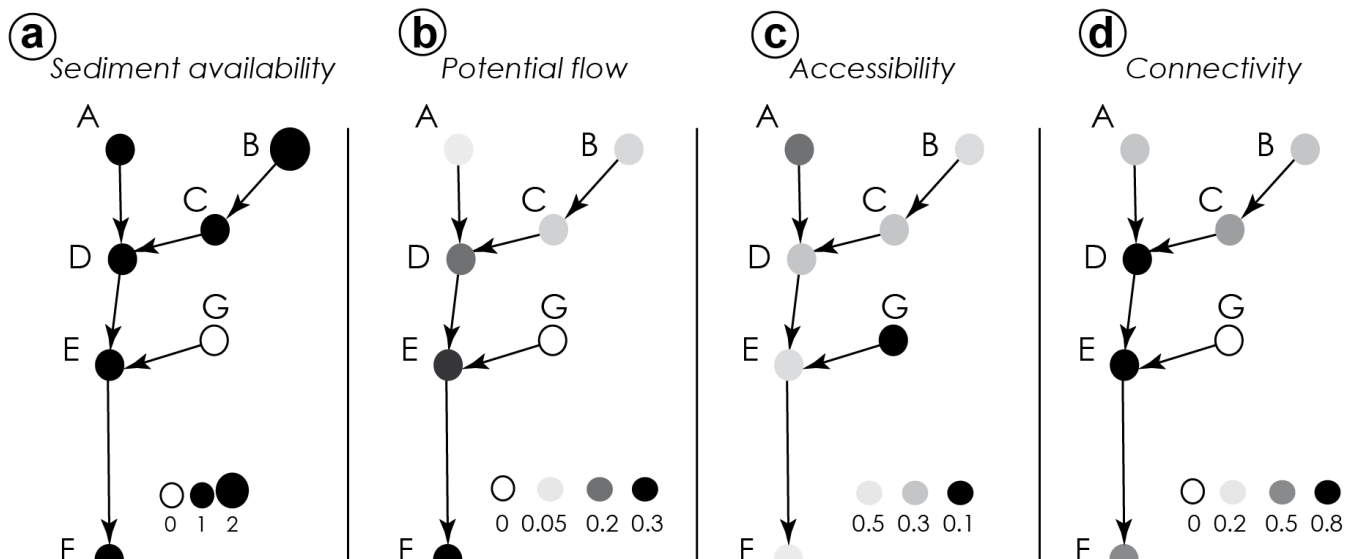


Figure 3: Assessment of the accessibility index within the virtual sediment cascade.

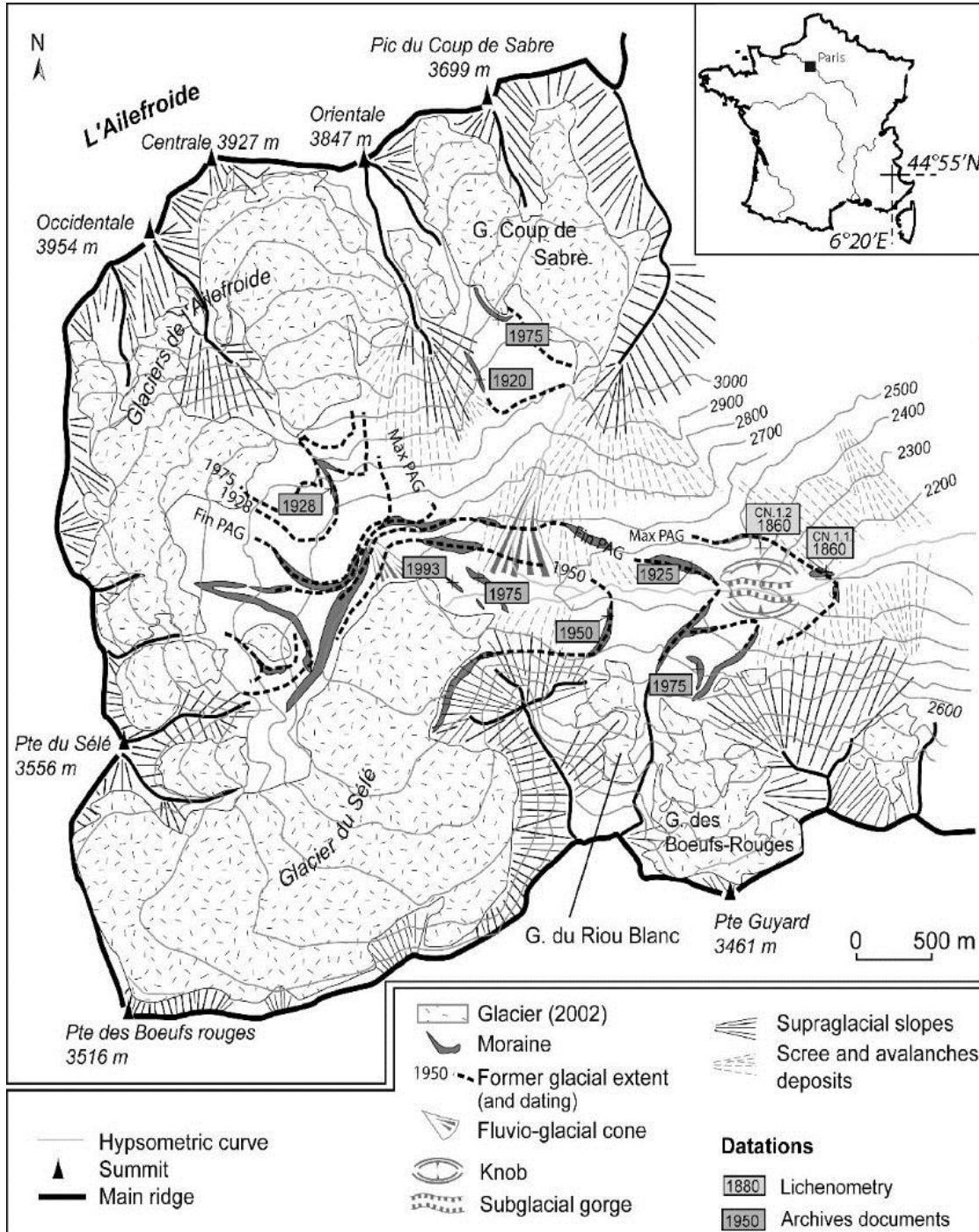


2 **Figure 4: Assessment of the connectivity index within the virtual sediment cascade.**

3
4

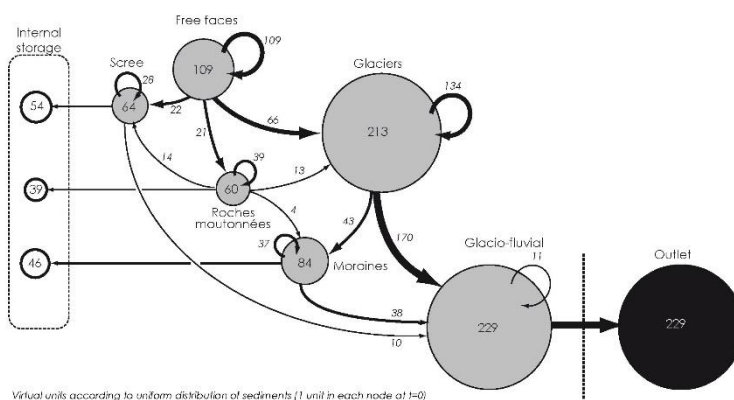
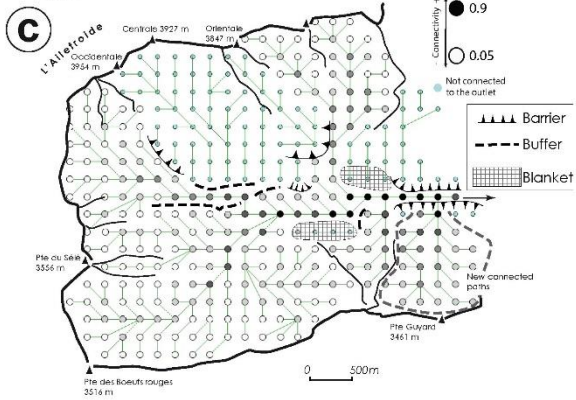
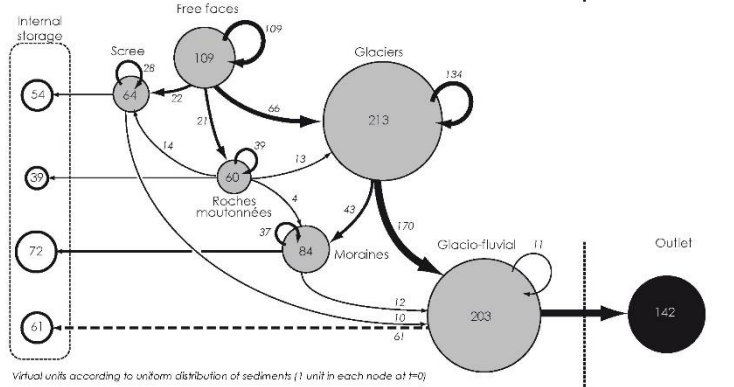
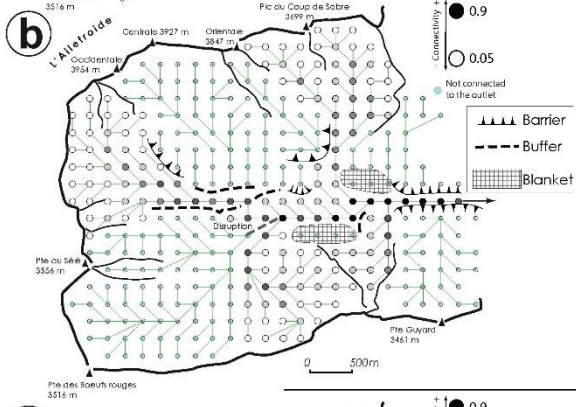
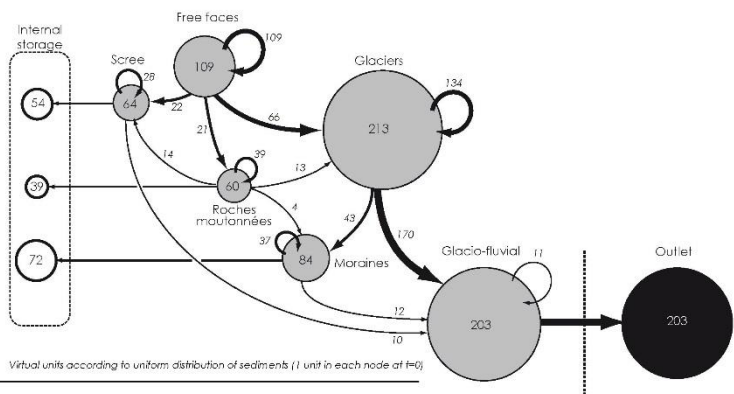
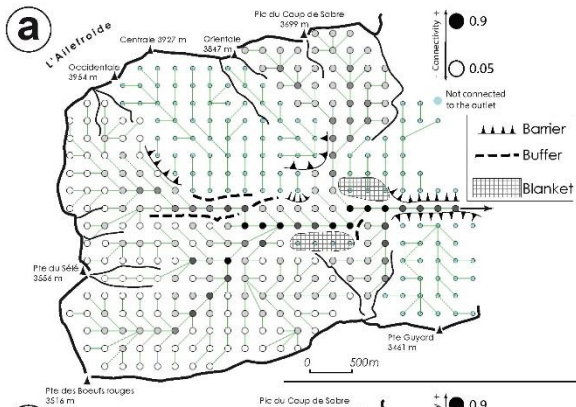


5
6 **Figure 5: Flow, accessibility and connectivity indices following a modified parameterization. Note how the connectivity of node D**
7 **is reinforced while the connectivity of F is reduced.**



1

2 **Figure 6: Geomorphological map of the study area: Celse-Nière catchment and sediment cascade.**



1

2 **Figure 7: Assessment of connectivity.** (a) Current structure of the cascade. (b) Connectivity map after the simulation of a
3 disruption at Séle toe. (c) Connectivity map after the simulation of a reconnection at Guyard outlet.

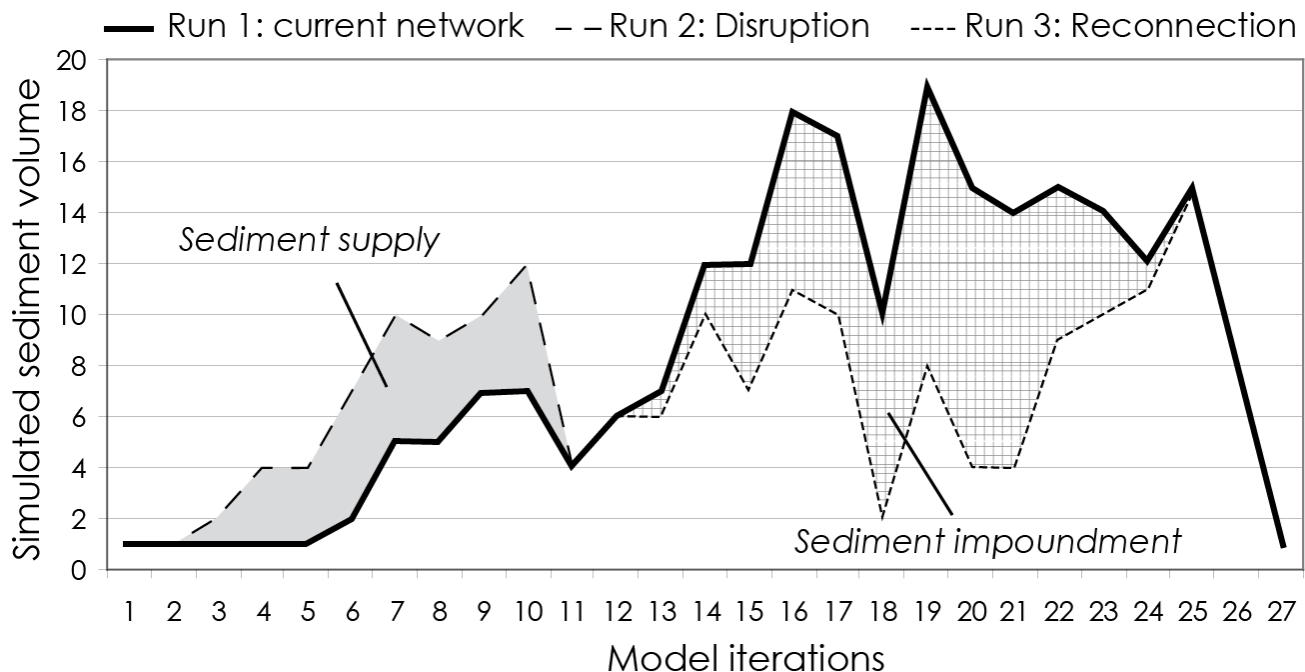
4

5

6

7

8



1

2 **Figure 8: Sedimentographs associated with runs 1, 2 and 3 on Celse-Nière catchment. Run 1 shows the current effect of the spatial**

3 **network structure on sediment waves, run 2 the potential impact of an edge disruption in a hotspot zone, and run 3 the potential**

4 **impact of a reconnection. Runs 1, 2 and 3 correspond to the graphs in Figure 7a, 7b, and 7c, respectively.**